

This article was downloaded by:[University of Washington]  
On: 15 September 2007  
Access Details: [subscription number 731869353]  
Publisher: Informa Healthcare  
Informa Ltd Registered in England and Wales Registered Number: 1072954  
Registered office: Mortimer House, 37-41 Mortimer Street, London W1T 3JH, UK



## Microcirculation

Publication details, including instructions for authors and subscription information:  
<http://www.informaworld.com/smpp/title~content=t713723262>

### A Theoretical Model for the Myogenic Response Based on the Length-Tension Characteristics of Vascular Smooth Muscle

Brian E. Carlson<sup>a</sup>, Timothy W. Secomb<sup>a</sup>

<sup>a</sup> Department of Physiology, University of Arizona, Tucson, Arizona, USA

Online Publication Date: 01 June 2005

To cite this Article: Carlson, Brian E. and Secomb, Timothy W. (2005) 'A Theoretical Model for the Myogenic Response Based on the Length-Tension Characteristics of Vascular Smooth Muscle', *Microcirculation*, 12:4, 327 - 338

To link to this article: DOI: 10.1080/10739680590934745

URL: <http://dx.doi.org/10.1080/10739680590934745>

PLEASE SCROLL DOWN FOR ARTICLE

Full terms and conditions of use: <http://www.informaworld.com/terms-and-conditions-of-access.pdf>

This article maybe used for research, teaching and private study purposes. Any substantial or systematic reproduction, re-distribution, re-selling, loan or sub-licensing, systematic supply or distribution in any form to anyone is expressly forbidden.

The publisher does not give any warranty express or implied or make any representation that the contents will be complete or accurate or up to date. The accuracy of any instructions, formulae and drug doses should be independently verified with primary sources. The publisher shall not be liable for any loss, actions, claims, proceedings, demand or costs or damages whatsoever or howsoever caused arising directly or indirectly in connection with or arising out of the use of this material.

# A Theoretical Model for the Myogenic Response Based on the Length–Tension Characteristics of Vascular Smooth Muscle

BRIAN E. CARLSON AND TIMOTHY W. SECOMB

Department of Physiology, University of Arizona, Tucson Arizona, USA

## ABSTRACT

**Objective:** A theoretical model is developed to describe the myogenic response of resistance vessels to changes in intravascular pressure, based on a consideration of the active and passive length–tension characteristics of vascular smooth muscle (VSM). The dependence of model parameters on vessel diameter is examined.

**Methods:** The vessel wall is represented mechanically as a nonlinear passive component in parallel with an active contractile component. The level of VSM tone is assumed to have a sigmoidal dependence on circumferential wall tension or stress. Model parameters are optimized for each of 18 independent experimental data sets previously obtained using pressure or wire myograph systems.

**Results:** Close fits between model predictions and experimental data are found in each case. An alternative formulation in which VSM tone depends on circumferential wall stress is found also to be consistent with available data. Significant trends in model parameters as a function of diameter are found.

**Conclusions:** The results support the hypothesis that circumferential tension or stress in the wall provides the signal for myogenic responses. The model provides a basis for simulating steady-state myogenic responses in vascular networks containing a range of vessel diameters.

*Microcirculation* (2005) **12**, 327–338. doi:10.1080/10739680590934745

**KEY WORDS:** arteriole, mathematical model, vascular regulation, vascular smooth muscle tone, vessel wall tension

Arterioles and small arteries are responsible for most of the peripheral resistance in the vasculature, and regulate blood flow acutely by dilating or constricting in response to several types of stimuli. These diameter changes are achieved by alterations in vascular smooth muscle (VSM) tone. One of the mechanisms responsible for a variation in VSM tone is the myogenic response, which is characterized by a vessel constriction occurring following an increase in intraluminal pressure. This response was first observed over 100 years ago when Bayliss noted changes in volume of the hindlimb of a dog after alteration of systemic blood pressure (1). Its significance was disputed until Folkow showed that vascular regulation

may have a myogenic component (15). Later work indicated that circumferential tension in the wall may be the control parameter governing the myogenic response (22). Much recent research has addressed the mechanisms responsible for the myogenic response at the cellular level (8,37).

Passive and maximally active length–tension characteristics of VSM were explored in several studies using in vitro wire (27,28,31) and pressure (7,32) myograph systems based on experimental methods developed by Bevan and Osher (2) and Duling et al. (13), respectively. Vessels were perfused with, or bathed in, activating (e.g., with norepinephrine) or relaxing ( $\text{Ca}^{2+}$ -free) physiological salt solutions, to allow determination of the minimal circumferential tension (passive component) and the maximally active tension (maximally active component) present in the vessel wall at a given circumferential length. In the referenced studies, only vessels developing spontaneous tone were included and no preconstrictors were used. Such results define the operating range of wall tension for a given vessel. Description of the

---

*This work was supported by NIH Grant HL70657 and by NSF Grant 9870659.*

*Address correspondence to Dr. T. W. Secomb, Department of Physiology, University of Arizona, Tucson AZ 85724-5051, USA. E-mail: secomb@u.arizona.edu*

*Received 19 May 2004; accepted 24 September 2004.*

---

myogenic response requires, in addition, information on the variation of VSM tone as intraluminal pressure is varied.

A number of studies have examined the myogenic response using pressure myograph systems (4,9,25,30,40,43). In these experiments, the level of VSM tone varied with intraluminal pressure, simulating the actual *in vivo* myogenic response. Vessels were perfused with physiological salt solutions that were assumed to have no effect on vascular tone. No precontractors were used and perfusion rates were low enough that effects of wall shear stress could be neglected. Diameter changes in resistance vessels (small arteries and arterioles in the diameter range of 25–250  $\mu\text{m}$ ) were recorded over a range of intraluminal pressures. In some cases, pressure was measured in a tube connected to the vessel. At the very low flow rates used, this pressure can be assumed to approximate intraluminal pressure. These experimental results indicate that the variation of diameter with pressure in a vessel exhibiting the myogenic response can be roughly divided into 3 phases (33). In the first phase, at low intraluminal pressures, a small increase in diameter is observed with increasing pressure. Occurring at intermediate values of intraluminal pressures, the second phase is characterized by a significant decrease in vessel diameter with increasing pressure. These 2 phases are described in all of the experimental studies utilized here, and encompass the range of conditions normally occurring *in vivo*. In a few of the studies (4,9,30,43), intraluminal pressures beyond the physiological range were applied, and vessel diameter was shown to increase with increasing pressure, representing the third phase of the myogenic response.

Previous theoretical models for the myogenic response have used a number of different approaches. In the model of Iida (20), the vessel wall elastic modulus is assumed to be a function of the intraluminal pressure. This model describes the form of the myogenic response at low and intermediate pressures accurately. However, passive and active components of wall tension are not distinguished, and the third, high-pressure phase of the myogenic response, which is dominated by the passive component, is not accurately represented. Fung proposed a model (16) in which passive and active components of the wall tension are represented. The passive component is effectively zero and the active component is maximal over the range of pressures considered. Although this model can reproduce observed active pressure responses (23), it does not reflect experimentally de-

termined length–tension relationships of maximally active VSM (7,27,28,31,32).

Several models incorporating variable VSM tone have been developed (5,14,44–46). VanBavel and Mulvany (44) recognized that VSM tone cannot depend solely on the agonist concentration of the perfusate but must depend on another variable, which they assumed to be vessel wall tension. Using wall tension as a parameter determining VSM tone is consistent with other studies (3,22,42). In their model (44), myogenic responses were not considered independently of agonist responses. In a model for flow regulation in the renal microcirculation, Feldberg et al. (14) represented the myogenic response by assuming that tone depends on intraluminal pressure according to a piecewise linear function. Cornelissen et al. (5) developed a model incorporating myogenic, flow-dependent, and metabolic control of coronary blood flow, but again myogenic tone was assumed to depend on intravascular pressure. None of these studies combined the length–tension characteristics of the vessel wall with tension-dependent generation of VSM tone in a model for the myogenic response. Recently, Yang et al. (45,46) developed a model for the myogenic response based on a consideration of intracellular signaling pathways in VSM cells. Wall tension was used as the primary mechanical variable influencing cellular activation.

The aim of the present study is to develop a theoretical model that describes the myogenic response of resistance vessels to intravascular pressure, based on a consideration of vascular smooth muscle mechanics, and assuming variable VSM tone. Following an increase in intravascular pressure, a vessel typically shows first an immediate passive increase in diameter, and then an active myogenic contraction to a new equilibrium diameter. The model describes this steady-state condition. Circumferential wall tension and wall stress are considered as potential variables determining the level of VSM tone. Model predictions are compared with experimental data from a number of studies, and the dependence of model parameters on vessel diameter is explored. The resulting model is designed to be used as part of more comprehensive models of blood flow regulation in vascular networks.

## METHODS

### Model Foundation

The vessel wall under tension is represented mechanically as a nonlinear spring and a contractile unit in

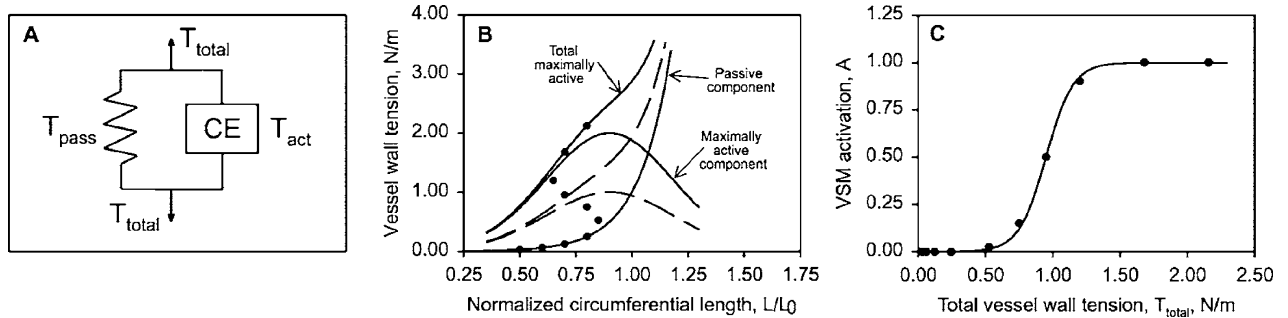


**Figure 1.** Graphical representation of model concepts. (A) Spring and contractile element representation of vessel wall response. (B) Vessel wall tension as a function of circumferential length. Solid curves show passive tension  $T_{pass}$ , maximally active tension  $T_{act}^{max}$ , and total maximally active tension  $T_{pass} + T_{act}^{max}$ . Dashed curves show active tension and total tension at 50% activation ( $A = 0.5$ ). Dots show typical observed behavior during active pressure response, with activation increasing as tension increases. (C) Representative example of variation of activation with tension, showing data points and fitted curve.

parallel (12) (Figure 1A). The maximal tension that can be generated at a given length is the sum of the passive (nonlinear spring) and maximally active VSM (contractile unit) components and is described here as the total maximally active tension. The minimal tension occurs when the contractile unit is inactive and is equivalent to the passive component of tension. In a partially activated vessel, the total vessel wall tension is

$$T_{total} = T_{pass} + A \cdot T_{act}^{max} \quad (1)$$

where  $T_{pass}$  is the passive component of tension,  $T_{act}^{max}$  is the maximal active component of tension, and  $A$ , the activation, represents the level of VSM tone, which varies between 0 and 1.

### Passive Component of Tension

Measured passive length–tension relationships (4,7,9,25,27,28,30–32,40,43) are nonlinear, with tension increasing rapidly at higher levels of circumferential stretch. The following exponential form is used to represent the passive tension component:

$$T_{pass}(L) = C_{pass} \exp \left[ C'_{pass} \left( \frac{L}{L_0} - 1 \right) \right] \quad (2)$$

where  $L$  is the vessel circumference,  $C_{pass}$  is the passive tension at a length of  $L_0$ , and  $C'_{pass}$  determines the steepness of the exponential curve. The reference length  $L_0$  is defined as  $\pi D_0$ , where  $D_0$  is the passive diameter of the vessel at an intraluminal pressure of

100 mmHg. Choice of a different  $L_0$  would yield an equivalent curve with appropriate changes in  $C_{pass}$  and  $C'_{pass}$ .

### Maximally Active Component of Tension

The total maximal tension was measured in length–tension studies (7,27,28,31,32) by bathing or perfusing the tissue with a maximally activating physiological salt solution. In some previous studies (11,35), a reduction in active tension observed at large circumferential lengths was attributed to cellular damage. However, Mulvany and Warshaw (28) showed that cellular integrity was maintained even at large circumferential stretch and that the decreasing active tension observed at these lengths was due to the properties of the VSM contractile apparatus. The maximal active component of tension can therefore be obtained by subtracting the passive component from the total maximal tension. The general form of the maximal active component in each study was similar to that observed in skeletal muscle, in which maximal tension is generated at a specific length and tension decreases symmetrically above and below this length (19). This behavior was modeled by a Gaussian curve:

$$T_{act}^{max}(L) = C_{act} \exp \left[ - \left( \frac{L/L_0 - C'_{act}}{C''_{act}} \right)^2 \right] \quad (3)$$

where  $C_{act}$ ,  $C'_{act}$ , and  $C''_{act}$  are parameters representing peak magnitude, relative peak location, and relative curve width, respectively, as shown in Figure 1B.

### VSM Tone

Circumferential wall tension, wall stress, strain, and pressure are potential determinants of VSM activation. Here, activation is assumed to depend on wall tension; other possibilities are considered below. Previous studies (14, 44) suggest that the dependence is sigmoidal, and the following expression was therefore used:

$$A(T_{\text{total}}) = \frac{1}{1 + \exp(-C_{\text{tone}} T_{\text{total}} + C'_{\text{tone}})} \quad (4)$$

where  $C_{\text{tone}}$  and  $C'_{\text{tone}}$  determine the steepness of the sigmoidal curve and tension at half-maximal activation. An example of the variation of  $A$  with wall tension is shown in Figure 1C. The assumed dependence of activation on tension implies that wall tension is controlled by a negative feedback mechanism (22). Increased tension causes increased tone and contraction, which reduces wall tension for a given transmural pressure according to the law of Laplace. The gain of this feedback system increases with increasing values of the parameter  $C_{\text{tone}}$ .

### Pressure, Tension, and Stress

The length–tension relationship of the vessel wall is related to the pressure–diameter response observed in pressure myograph studies through the law of Laplace:

$$T_{\text{total}} = \frac{PD}{2} \quad (5)$$

assuming that the vessel wall thickness is much less than the radius. The corresponding circumferential wall stress is

$$\sigma_{\text{total}} = T_{\text{total}}/w = \frac{PD}{2w} \quad (6)$$

where  $w$  is the wall thickness. For the model in which activation depends on wall stress rather than tension,  $\sigma_{\text{total}}$  replaces  $T_{\text{total}}$  in Equation 4.

### Optimization and Evaluation of Model Parameters

For given values of the 7 model parameters,  $C_{\text{pass}}$ ,  $C'_{\text{pass}}$ ,  $C_{\text{act}}$ ,  $C'_{\text{act}}$ ,  $C''_{\text{act}}$ ,  $C_{\text{tone}}$ , and  $C'_{\text{tone}}$ , Equations 1–5 and the relationship  $L = \pi D$  implicitly define the dependence of vessel diameter on pressure both in the

passive state and when an active myogenic response is present. An optimization procedure is used to find the parameter values that minimize the mean square deviation between the predicted and measured diameters at the given values of intraluminal pressure, using the downhill simplex method (29). First, the 2 passive component parameters,  $C_{\text{pass}}$  and  $C'_{\text{pass}}$ , are estimated for best fit to the passive data. This optimization shows rapid convergence to consistent parameter values, for a range of initial guesses. Then, the remaining parameters,  $C_{\text{act}}$ ,  $C'_{\text{act}}$ ,  $C''_{\text{act}}$ ,  $C_{\text{tone}}$ , and  $C'_{\text{tone}}$ , are estimated for best fit to the active pressure data. The predicted diameter values are only defined implicitly by Equations 1–5; therefore a hybrid secant-bisection root-finding algorithm is used to calculate the diameters at each pressure value. The results of this optimization are found to be sensitive to the initial parameter guesses, indicating the presence of local minima in the mean deviation. Therefore, whenever the optimization procedure approaches a minimum, a perturbation is applied and the process repeated to test whether the minimum is local or global. To avoid unrealistic values of the model parameters, all parameters are constrained to remain positive.

This 7-parameter optimization procedure was applied to 5 data sets from 4 studies (4,9,30,43) that contain data from all 3 response phases, including the high-pressure response. Five other data sets from 2 studies (25,40) lack data in the third phase of the myogenic response and as a result do not provide sufficient information to uniquely define the maximal active component of tension. Therefore, a reliable estimation of parameters requires a reduction in the degrees of freedom of the model. To achieve this, we utilize length–tension data from 5 studies (7,27,28,31,32) to establish values for  $C_{\text{pass}}$ ,  $C'_{\text{pass}}$ ,  $C_{\text{act}}$ ,  $C'_{\text{act}}$ , and  $C''_{\text{act}}$  by fitting Equations 2 and 3 to the passive and maximally active tension data, using similar procedures to those already described. As discussed below,  $C'_{\text{act}}$  and  $C''_{\text{act}}$  do not vary significantly with vessel diameter over the range of 50–300  $\mu\text{m}$ . For the 5 data sets lacking data on the high-pressure response, these 2 parameters were set equal to the average of the values obtained from the length–tension studies, and the remaining 5 parameters were estimated using the procedure already described. These model results are referred to as 5-parameter optimizations.

Only one of the studies (4) used in our analysis recorded the vessel wall thickness at a specified vessel diameter. Data from this study were used to test

the model in which activation depends on wall stress rather than tension. The 7-parameter optimization was performed as before, but with  $\sigma_{\text{total}}$  replacing  $T_{\text{total}}$  in Equation 4.

## RESULTS

### Optimization and Model Parameters

In Figure 2, model results are compared with experimental data for 5 data sets (4,9,30,43). The left column of graphs displays the experimental active pressure and passive data and the model fits in terms of pressure and diameter, the measured quantities. At low pressures, VSM activation is zero or small, and diameters are close to passive values. At intermediate pressures, above  $\sim 40$  mmHg, activation increases and diameters decrease. At high pressures, the VSM is already fully activated and additional increases in pressure cause distension of the vessel. All 3 phases of vessel response are fit closely by this model, with root mean square (RMS) deviations varying from 1.61 to 4.60% over the 5 data sets. Corresponding parameter values are given in Table 1. The middle column of graphs presents the same data as length–tension relationships. Curves representing the maximally active component of tension and the maximally active total tension are also included. The active pressure response, with VSM tone varying from passive to maximally active, appears as an S-shaped curve. The importance of the data points at high tension levels (at the top of the S) in establishing the maximally active component of tension curve is evident. The right column of graphs shows the variation of VSM tone with total vessel wall tension. In this case, the data points are deduced from the experimental data and the fitted maximally active and passive tension curves. VSM tone exhibits a steep increase with tension above a certain threshold.

Table 1 also includes parameter values estimated using 8 data sets from length–tension studies (7,27,28,31,32) and from 5 data sets lacking data for the high-pressure, third phase of the myogenic response (25,40). In the length–tension studies, vessels were passive or fully activated, so corresponding values of  $C_{\text{tone}}$  and  $C'_{\text{tone}}$ , could not be estimated. RMS deviations for the fit of the maximally active component of tension data varied from 2.44 to 9.31%. For the sets lacking high-pressure data,  $C'_{\text{act}}$  and  $C''_{\text{act}}$  could not be deduced from the pressure–diameter data, as previously discussed, and were set equal to the average of the values obtained from

the length–tension experiments, i.e.,  $C'_{\text{act}} = 0.910$  and  $C''_{\text{act}} = 0.374$ . The quality of the resulting 5-parameter fits to the pressure–diameter data is similar to that for the cases shown in Figure 2, with RMS deviations varying from 0.65 to 8.45%.

### Dependence of Parameters on Vessel Diameter

Estimated parameter values from all data sets considered are shown in Figure 3 as functions of the reference vessel diameter,  $D_0$ . Although this does not necessarily represent an in vivo vessel diameter, it is a useful relative measure. Values for  $C'_{\text{pass}}$ , which indicates the steepness of the passive response curve, show a significant ( $p < .05$ ) negative trend with respect to increasing diameter (Figure 3A). The smallest values for  $C'_{\text{pass}}$  are obtained in experiments utilizing a wire myograph. The parameter  $C_{\text{act}}$ , which represents the peak magnitude of the maximally active response, increases significantly with increasing diameter (Figure 3B). The parameter  $C_{\text{tone}}$ , which defines the dependence of tone on wall tension, shows a significant decrease with increasing diameter (Figure 3C). The dependence on diameter of the remaining parameters,  $C_{\text{pass}}$ ,  $C'_{\text{act}}$ ,  $C''_{\text{act}}$ , and  $C_{\text{tone}}$ , is not shown. The passive tension  $C_{\text{pass}}$  at the reference diameter, corresponding to an intravascular pressure of 100 mmHg, increases linearly with diameter as expected from the law of Laplace, Equation 5. The other parameters,  $C'_{\text{act}}$ ,  $C''_{\text{act}}$ , and  $C'_{\text{tone}}$ , show no significant dependence on reference vessel diameter over the range of vessel sizes considered here.

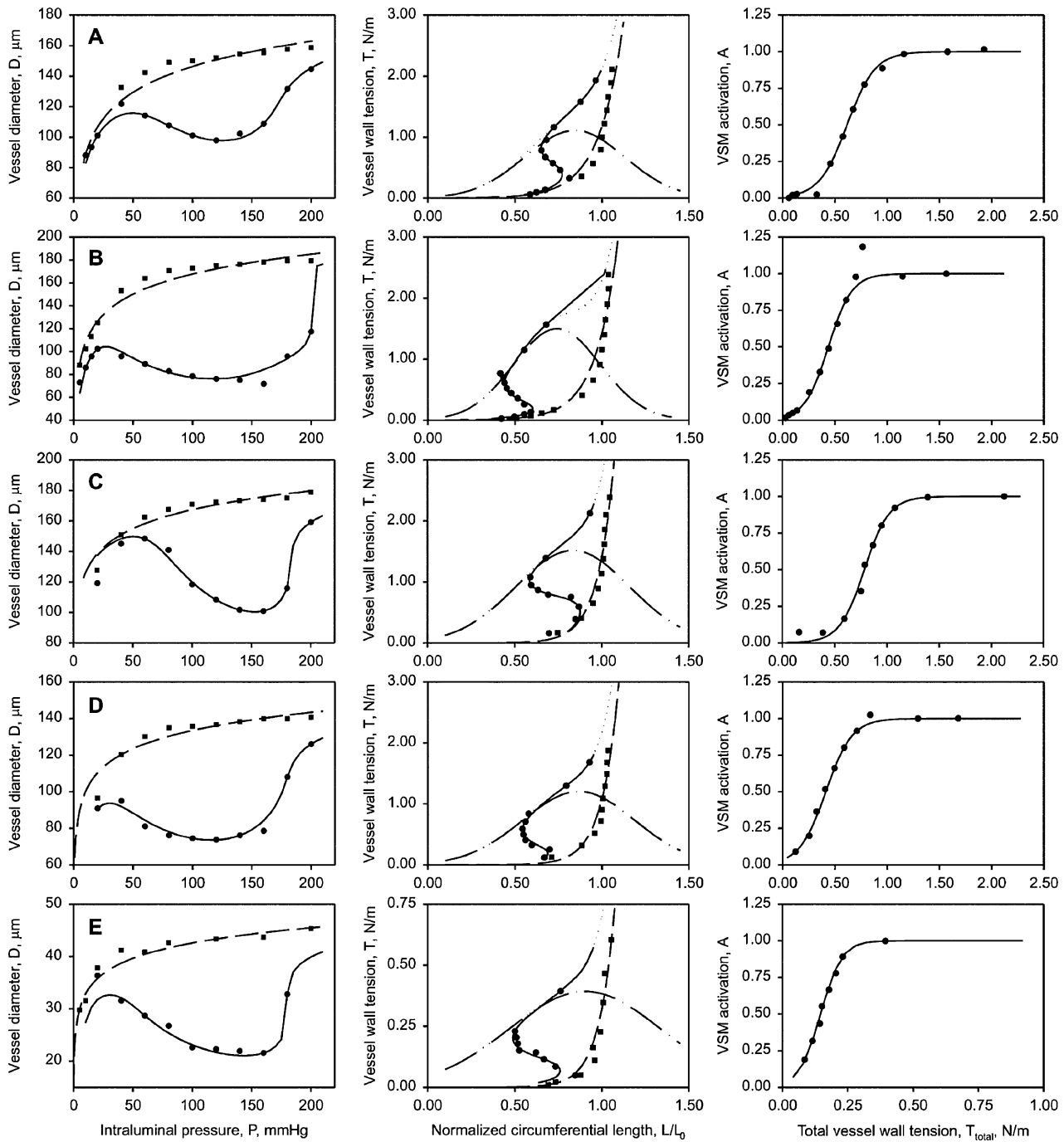
### Results with Stress-Dependent Activation

Two data sets (4) were used to test the model in which activation depends on wall stress rather than tension. Figure 4 shows the resulting optimized fits in the same form as in Figure 2. The closeness of fit between the model and the data is similar in the 2 formulations (Figures 2A, B and 4A, B). For the femoral artery data, the model curves and parameters differ appreciably between the 2 formulations, due to a difference in the peak height, location and width of the maximally active VSM stress curve (Table 1).

## DISCUSSION

### Agreement Between Model and Observations

Five available sets of experimental pressure–diameter data (4,9,30,43) allowed optimization of all 7 parameters in the model. The resulting model curves



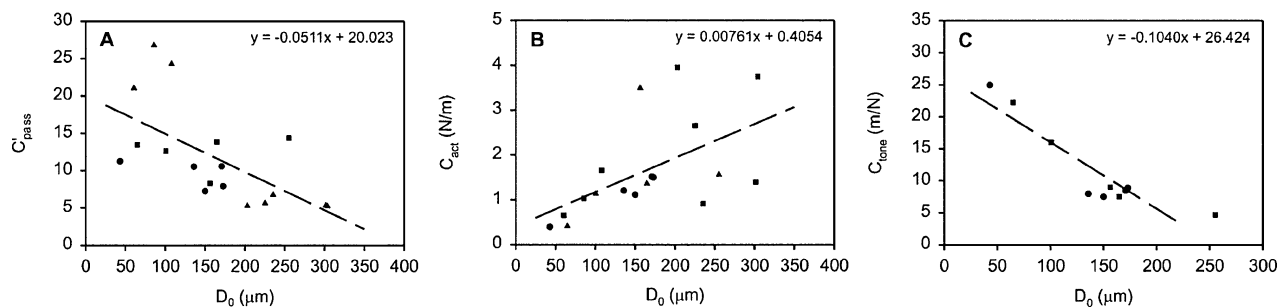
**Figure 2.** Pressure–diameter, length–tension, and activation curves: comparison of experimental and model results. Experimental data are from the following sources: (A) rat mesenteric arterioles (4); (B) rat femoral arterioles (4); (C) rat skeletal muscle arterioles (30); (D) rat adipose tissue arterioles (43); (E) hamster cheek pouch arterioles (9). Left column: experimental data (■, passive; ●, active) and model results (---, passive; —, active) in terms of pressure and diameter. Middle column: experimental data (■, passive; ●, active) and model results (---, passive; —, active) in terms of length and tension, including predicted maximally active VSM tension (-·-) and maximally active total tension (···). Right column: predicted curves and inferred experimental data for VSM activation level as a function of total vessel wall tension.

Table 1. Model parameter values

Reference	Species and vessel type	$D_p$ ( $\mu\text{m}$ ) at 100 mmHg	$C_{\text{pass}}$ (N/m)	$C'_{\text{pass}}$	$C_{\text{act}}$ (N/m)	$C'_{\text{act}}$	$C''_{\text{act}}$	$C_{\text{tone}}$ (m/N)	$C'_{\text{tone}}$	RMS deviation <sup>c</sup> (%)
(4)	Rat mesenteric [7]	150.0	1.168	7.240	1.108	0.843	0.406	7.479	4.614	1.89
(4)	Rat mesenteric [7] <sup>d</sup>	150.0	1.168	7.240	1.103	0.853	0.418	0.0853 <sup>d</sup>	6.099	1.61
(4)	Rat femoral [7]	172.8	1.416	7.901	1.499	0.742	0.353	8.871	3.881	3.94
(4)	Rat femoral [7] <sup>d</sup>	172.8	1.416	7.901	1.858	0.958	0.562	0.147 <sup>d</sup>	4.088	3.34
(30)	Rat skeletal muscle [13]	170.8	1.386	10.568	1.514	0.834	0.463	8.462	6.640	3.79
(43)	Rat adipose tissue [6]	135.8	1.067	10.516	1.202	0.867	0.455	7.973	3.296	1.88
(9)	Hamster cheek pouch [8]	43.0	0.316	11.247	0.392	0.903	0.618	24.934	3.631	4.60
Seven-parameter fits <sup>a</sup>										
(28)	Rat mesenteric [8]	230.0	1.697	5.298	3.955	0.950	0.471	—	—	6.54
(27)	Rat mesenteric [1]	225.6	1.417	5.628	2.649	0.962	0.520	—	—	6.02
(31)	Rat coronary [6]	301.6	1.672	5.324	1.395	0.908	0.416	—	—	2.58
(31)	Rat mesenteric [6]	304.1	1.857	5.226	3.748	0.842	0.375	—	—	2.44
(7)	Hamster cheek pouch [7]	108.1	0.843	24.279	1.655	0.998	0.359	—	—	6.30
(7)	Hamster cheek pouch [11]	85.7	0.655	26.785	1.024	0.852	0.276	—	—	9.31
(7)	Hamster cheek pouch [3]	60.7	0.371	21.035	0.654	0.813	0.214	—	—	8.48
(32)	Bovine retinal [6]	235.6	1.802	6.782	0.908	0.956	0.364	—	—	4.53
Length-tension fits <sup>b</sup>										
Five-parameter fits <sup>c</sup>										
(40)	Rat cremaster muscle [8]	156.5	1.043	8.293	3.491	0.910	0.374	9.018	4.631	8.45
(25)	Porcine coronary [9]	255.4	1.719	14.354	1.564	0.910	0.374	4.674	2.940	1.96
(25)	Porcine coronary [16]	164.8	1.141	13.828	1.360	0.910	0.374	7.508	2.978	1.08
(25)	Porcine coronary [26]	100.8	0.687	12.606	1.131	0.910	0.374	15.977	4.180	0.65
(25)	Porcine coronary [7]	64.9	0.459	13.431	0.405	0.910	0.374	22.252	2.874	2.27

<sup>a</sup>Data sets including three phases of response.<sup>b</sup>Data sets with passive and maximally active vessels.<sup>c</sup>Data sets including two phases of response.<sup>d</sup>Parameter values obtained assuming activation is a function of total wall stress. Unit of  $C_{\text{tone}}$  is  $\text{m}^2/\text{N}$ .<sup>e</sup>RMS deviations refer to active response data in five- and seven-parameter fits and to maximally active component of tension in length-tension fits.

Note. Values in brackets: number of vessels in sample.



**Figure 3.** Variation of model parameters with reference diameter of vessel, for the data sets considered. (A) Passive tension parameter  $C'_{\text{pass}}$ . (B) Active tension parameter  $C_{\text{act}}$ . (C) VSM tone parameter  $C_{\text{tone}}$ . Dashed lines represent linear regressions. Equations of regression lines are included in each graph.

represent all these data sets with remarkable accuracy (Figure 2, left column). A similar quality of fit was obtained for data sets lacking data in the high-pressure range (25,40), with values for 2 parameters representing the position and width of the maximal active tension curve derived from independent length–tension data. The resulting fitted values of the remaining 5 parameters are in a similar range to those obtained from the 7-parameter optimizations. Thus, this model appears to provide an adequate description of the myogenic response over the range of vessel sizes, tissue types, and species in the studies utilized here, and unifies a substantial body of experimental data.

### Parameter Dependence on Vessel Diameter

The dependence of 3 of the model parameters on reference vessel diameter is shown in Figure 3. The significant decrease in  $C'_{\text{pass}}$  with increasing diameter implies that the smaller vessels are relatively stiffer than the larger vessels investigated, as observed previously (17). The parameter  $C_{\text{act}}$  representing the peak magnitude of the maximally active tension shows a significant positive correlation with diameter. This is to be expected because vessel wall thickness, and hence the number and/or size of force-generating smooth muscle cells, increases with increasing diameter.

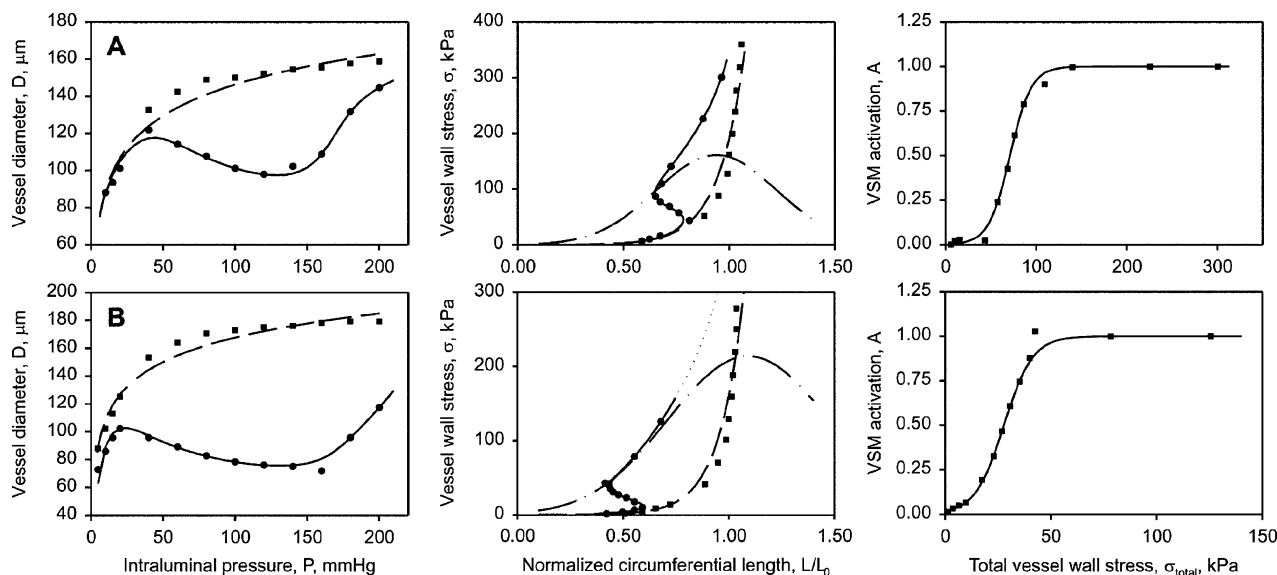


**Figure 4.** Pressure–diameter, length–stress, and activation curves describing the two three-phase data sets that include reference wall thickness data, analyzed assuming that activation is a function of total wall stress. (A) Rat mesenteric arterioles ( $\dagger$ ). (B) Rat femoral arterioles ( $\dagger$ ). Left column: experimental data and model results in terms of pressure and diameter. Middle column: experimental data and model results in terms of length and stress, including predicted maximally active VSM stress and maximally active total stress. Right column: predicted curves and inferred experimental data for the VSM activation level as a function of total vessel wall stress.

The parameters  $C'_{\text{act}}$  and  $C''_{\text{act}}$  establish the location and width of the maximally active tension curve with respect to vessel circumference. Neither shows significant dependence on reference vessel diameter. These results suggest that VSM cells show similar relationships between length and active tension in vessels with reference diameters ranging from about 50 to 300  $\mu\text{m}$ . Values of  $C'_{\text{act}}$  are close to 1 (Table 1), indicating that the peak force generation occurs at a length close to that at which significant passive tension is generated in the vessel wall. This contrasts with striated muscle, where peak force is generated when the muscle cell is substantially shorter than the length needed to generate significant passive tension in the cell and its surrounding extracellular matrix (41).

The parameter  $C_{\text{tone}}$  describes the sensitivity of tone to changes in tension. With increasing reference diameter,  $C_{\text{tone}}$  decreases. This trend is consistent with the fact that larger vessels have thicker walls and more load-bearing VSM cells. The parameter,  $C_{\text{tone}}$ , would be expected to be smaller if the tension is distributed over a larger number of VSM cells. It would be desirable to express the activation as a function of tension per VSM cell, but the studies considered here do not include sufficient data on wall morphology to make this possible.

Parameter values show significant variations that cannot be fully accounted for by a dependence on diameter (Figure 3 and Table 1). Some of this variability may result from the fact that the experimental results used are derived from several different animal species and tissue types (Table 1). Also, results obtained using a wire myograph may not correspond with those obtained with a pressure myograph apparatus (24). In the pressure myograph, the vessel can be held at constant length, mimicking the situation in vivo. In the wire myograph, vessel length may change with loading or contraction. However, the available data sets are not sufficient to reveal systematic variations in model parameters with species, tissue type or experimental method used.

### Factors Determining Activation

Initiation of smooth muscle cell contraction is linked to the flux of calcium across the cell membrane (37). This calcium influx initiates signaling pathways, leading to release of stored calcium, myosin light-chain phosphorylation, and contraction of the actin-myosin complex. The mechanical factors and mechanisms triggering increased intracellular calcium con-

centration,  $[\text{Ca}^{2+}]_i$ , have not been definitely identified. Proposed mechanical factors include strain, pressure, tension, and stress, and proposed mechanisms include stretch activation of transmembrane channels, depolarization of the stretched membrane, integrin-modulated transduction of tension, and secondary messenger alteration of the contractile protein  $[\text{Ca}^{2+}]_i$  sensitivity (8).

Dependence of VSM activation on VSM strain (i.e., degree of elongation) has been frequently proposed since the discovery of stretch-activated calcium channels and stretch depolarization of the cell membrane. However, the experimental results show that VSM strain cannot be the main controlling variable for activation, since multiple levels of activation can occur at a given level of vessel strain, as in the S-shaped part of the active length-tension curves (Figure 2, middle column). Additionally, if strain were the controlling variable, an increase in pressure could lead to a contraction tending to restore the vessel to its original diameter, but could not result in a decrease in diameter, as seen in the myogenic response. These arguments indicate that although stretch-activated channels may play a role in the myogenic response, VSM strain itself cannot be the main controlling variable. This is consistent with the finding that  $[\text{Ca}^{2+}]_i$  levels are not related directly to VSM strain (47), and does not exclude the possibility that wall tension or stress is sensed by changes in strain in a passive sensing element coupled in series with the contractile elements of a smooth muscle cell (22).

Intravascular pressure has been used in some models as the parameter determining VSM tone (5,6,14). However, this is unlikely to be a valid assumption for several reasons. First, the stress due to pressure is much smaller than the circumferential stress in a thin-walled vessel, as can be seen from Equation 6. Second, sensing of the transmural pressure difference would require VSM cells to detect the differential pressure between their inner and outer surfaces, and there is no evidence for such a pressure sensing mechanism in VSM cells. Thirdly, such a mechanism would require that the level of activation varies smoothly with pressure in some ranges but varies abruptly in other ranges, based on experimental observations (Figure 2, left column). In contrast, mechanisms based on a smooth dependence on wall tension or stress (present model) inherently lead to such behavior.

Our results support the hypothesis that circumferential wall tension or stress is the primary variable

governing VSM activation. Tension in VSM cells may be transmitted via the cytoskeleton to integrins, which can influence the signaling cascade leading to contraction (10,26). Tension has been positively correlated to  $[Ca^{2+}]_i$  and myosin light chain phosphorylation, both critical events in the contraction of smooth muscle (47). The present model shows that a sigmoidal variation in VSM tone as a function of tension is compatible with the myogenic responses observed in all the studies considered.

Wall stress is closely related to wall tension, according to Equation 6. Estimation of wall stress requires data on wall thickness, which is not available for most of the studies considered here. For the data of Bund (4), a model based on the assumption that activation depends on stress gave essentially equivalent results to the model based on tension. Therefore, it is not possible to distinguish between these two possibilities based on the available experimental evidence. For purposes of simulating regulatory mechanisms, the model based on wall tension appears to be adequate and can be used without information on wall thickness.

### Hysteresis in Myogenic Response Behavior

Unstable resistance vessel diameters have been observed in some studies, with more than one possible radius at a given pressure and hysteretic behavior during loading and unloading (7,18,21,34,38,39). In the present model, the possibility of such behavior can be assessed with reference to the results shown in Figure 2 (middle column). According to Equation 5, a given intravascular pressure can be represented by a line through the origin with a slope proportional to the pressure. Multiple radii are possible if such a line intersects the active length–tension curve more than once. This occurs only in the upper range of pressures, if at all, in the examples considered here. For instance, such behavior is seen in the Bund (4) femoral artery data (Figure 2B, middle column) and is reflected in the abrupt transition in diameter predicted at a pressure of about 200 mmHg (left column). This phenomenon has been discussed by Quick et al. (36) for the case of vessels with fixed levels of VSM tone. According to the results of the present model, hysteresis would be expected to occur only at pressures above the normal physiological range.

### Applications of the Model

The present model has been developed based on current concepts of smooth muscle mechanics, and uses

a minimum number of free parameters to provide a close fit to experimental data. As such, it provides a consistent framework for comparing and interpreting data from several experimental studies. The variation of model parameters with diameter is expressed in terms of linear correlations, which can be used to predict the myogenic response of a vessel segment with any given diameter in the range considered, allowing the simulation of myogenic responses in networks of vessels. Effects of other signals, such as wall shear stress and vasoactive substances, can be incorporated into the model through their effects on the activation parameter  $A$ . The present model applies to steady-state conditions. It can be extended to simulate time-dependent components of the myogenic response by considering the dynamic dependence of the activation  $A$  on the time-varying tension  $T_{total}$ . The model can also be extended to incorporate more detailed models of intracellular signaling processes and cellular-level wall mechanics, as have recently been presented (45,46).

### REFERENCES

1. Bayliss WM. (1902). The local reactions of the arterial wall to changes of internal pressure. *J Physiol Lond* 28:220–231.
2. Bevan JA, Osher JV. (1972). Direct method for recording tension changes in wall of small blood-vessels in vitro. *Agents and Actions* 2:257–260.
3. Bulbring E. (1955). Correlation between membrane potential, spike discharge and tension in smooth muscle. *J Physiol Lond* 128:200–221.
4. Bund SJ. (2001). Spontaneously hypertensive rat resistance artery structure related to myogenic and mechanical properties. *Clin Sci* 101:385–393.
5. Cornelissen AJ, Dankelman J, VanBavel E, Spaan JA. (2002). Balance between myogenic, flow-dependent, and metabolic flow control in coronary arterial tree: a model study. *Am J Physiol Heart Circ Physiol* 282:H2224–H2237.
6. Cornelissen AJ, Dankelman J, VanBavel E, Stassen HG, Spaan JA. (2000). Myogenic reactivity and resistance distribution in the coronary arterial tree: a model study. *Am J Physiol Heart Circ Physiol* 278:H1490–H1499.
7. Davis MJ, Gore RW. (1989). Length–tension relationship of vascular smooth-muscle in single arterioles. *Am J Physiol Heart Circ Physiol* 256:H630–H640.
8. Davis MJ, Hill MA. (1999). Signaling mechanisms underlying the vascular myogenic response. *Physiol Rev* 79:387–423.
9. Davis MJ, Sikes PJ. (1990). Myogenic responses of isolated arterioles: test for a rate-sensitive mechanism. *Am J Physiol Heart Circ Physiol* 259:H1890–H1900.

10. Davis MJ, Wu X, Nurkiewicz TR, Kawasaki J, Davis GE, Hill MA, Meininger GA. (2001). Integrins and mechanotransduction of the vascular myogenic response. *Am J Physiol Heart Circ Physiol* 280:H1427–H1433.
11. Dobrin PB. (1973). Influence of initial length on length–tension relationship of vascular smooth-muscle. *Am J Physiol* 225:664–670.
12. Dobrin PB. (1978). Mechanical properties of arteries. *Physiol Rev* 58:397–460.
13. Duling BR, Gore RW, Dacey RG, Damon DN. (1981). Methods for isolation, cannulation, and invitro study of single micro-vessels. *Am J Physiol* 241:H108–H116.
14. Feldberg R, Colding-Jorgensen M, Holstein-Rathlou NH. (1995). Analysis of interaction between TGF and the myogenic response in renal blood-flow autoregulation. *Am J Physiol Renal Physiol* 269:F581–F593.
15. Folkow B. (1949). Intravascular pressure as a factor regulating the tone of the small vessels. *Acta Physiol Scand* 17:289–310.
16. Fung YC. (1997). *Biomechanics: Circulation*. New York: Springer-Verlag, 489–501.
17. Gore RW. (1972). Wall stress—determinant of regional differences in response of frog microvessels to norepinephrine. *Am J Physiol* 222:82–91.
18. Greenwald SE, Newman DL, Denyer HT. (1982). Effect of smooth-muscle activity on the static and dynamic elastic properties of the rabbit carotid-artery. *Cardiovasc Res* 16:86–94.
19. Herlihy JT, Murphy RA. (1973). Length–tension relationship of smooth-muscle of hog carotid-artery. *Circ Res* 33:275–283.
20. Iida N. (1989). Physical properties of resistance vessel wall in peripheral blood flow regulation, I: mathematical model. *J Biomech* 22:109–117.
21. Jackson PA, Duling BR. (1989). Myogenic response and wall mechanics of arterioles. *Am J Physiol Heart Circ Physiol* 257:H1147–H1155.
22. Johnson PC. (1980). The myogenic response. In: *Handbook of Physiology. The Cardiovascular System: Vascular Smooth Muscle* (DF Bohr, AP Somlyo, HV Sparks, Eds.). Bethesda, MD: American Physiological Society, 409–442.
23. Kuo L, Davis MJ, Chilian WM. (1990). Endothelium-dependent, flow-induced dilation of isolated coronary arterioles. *Am J Physiol Heart Circ Physiol* 259:H1063–H1070.
24. Lew MJ, Angus JA. (1992). Wall thickness to lumen diameter ratios of arteries from Shr and Wky: comparison of pressurized and wire-mounted preparations. *J Vasc Res* 29:435–442.
25. Liao JC, Kuo L. (1997). Interaction between adenosine and flow-induced dilation in coronary microvascular network. *Am J Physiol Heart Circ Physiol* 272:H1571–H1581.
26. Martinez-Lemus LA, Wu X, Wilson E, Hill MA, Davis GE, Davis MJ, Meininger GA. (2003). Integrins as unique receptors for vascular control. *J Vasc Res* 40:211–233.
27. Mulvany MJ. (1984). Determinants of vascular hemodynamic characteristics. *Hypertension* 6:13–18.
28. Mulvany MJ, Warshaw DM. (1979). The active tension-length curve of vascular smooth muscle related to its cellular components. *J Gen Physiol* 74:85–104.
29. Nelder JA, Mead R. (1965). A simplex-method for function minimization. *Comput J* 7:308–313.
30. New DI, Chesser AMS, Raftery MJ, Yaqoob MM. (2003). The myogenic response in uremic hypertension. *Kidney Int* 63:642–646.
31. Nyborg NCB, Baandrup U, Mikkelsen EO, Mulvany MJ. (1987). Active, passive and myogenic characteristics of isolated rat intramural coronary resistance arteries. *Pflügers Arch Archiv* 410:664–670.
32. Nyborg NCB, Korsgaard N, Nielsen PJ. (1990). Active wall tension–length curve and morphology of isolated bovine retinal small arteries: important feature for pharmacodynamic studies. *Exp Eye Res* 51:217–224.
33. Osol G, Brekke JF, McElroy-Yaggy K, Gokina NI. (2002). Myogenic tone, reactivity, and forced dilatation: a three-phase model of in vitro arterial myogenic behavior. *Am J Physiol Heart Circ Physiol* 283:H2260–H2267.
34. Pascale K. (1989). Bidimensional passive and active mechanical-behavior of rat tail artery segments in vitro. *Basic Res Cardiol* 84:442–448.
35. Peterson JW, Paul RJ. (1974). Effects of initial length and active shortening on vascular smooth-muscle contractility. *Am J Physiol* 227:1019–1024.
36. Quick CM, Baldick HL, Safabakhsh N, Lenihan TJ, Li JKI, Weizsacker HW, Noordergraaf A. (1996). Unstable radii in muscular blood vessels. *Am J Physiol Heart Circ Physiol* 271:H2669–H2676.
37. Schubert R, Mulvany MJ. (1999). The myogenic response: established facts and attractive hypotheses. *Clin Sci* 96:313–326.
38. Speden RN. (1973). Maintenance of arterial constriction at different transmural pressures. *J Physiol Lond* 229:361–381.
39. Speden RN, Freckelton DJ. (1970). Constriction of arteries at high transmural pressures. *Circ Res* 27(Suppl II):99–112.
40. Sun D, Huang A, Koller A, Kaley G. (1995). Flow-dependent dilation and myogenic constriction interact to establish the resistance of skeletal muscle arterioles. *Microcirculation* 2:289–295.
41. ter Keurs HEDJ, Iwazumi T, Pollack GH. (1978). Sarcomere length–tension relation in skeletal-muscle. *J Gen Physiol* 72:565–592.
42. Thurau KWC. (1964). Autoregulation of renal blood flow and glomerular filtration rate including data on tubular and peritubular capillary pressures and vessel wall tension. *Circ Res* 15:132–141.

43. Undavia SS, Berger V, Kaley G, Messina EJ. (2003). Myogenic responses of isolated adipose tissue arterioles. *Microvasc Res* 66:140–146.
44. VanBavel E, Mulvany MJ. (1994). Role of wall tension in the vasoconstrictor response of cannulated rat mesenteric small arteries. *J Physiol Lond* 477:103–115.
45. Yang J, Clark JW, Bryan RM, Robertson C. (2003). The myogenic response in isolated rat cerebrovascu-  
lar arteries: smooth muscle cell model. *Med Eng Phys* 25:691–709.
46. Yang J, Clark JW, Bryan RM, Robertson CS. (2003). The myogenic response in isolated rat cerebrovascular arteries: vessel model. *Med Eng Phys* 25:711–717.
47. Zou H, Ratz PH, Hill MA. (1995). Role of myosin phosphorylation and  $[Ca^{2+}]_i$  in myogenic reactivity and arteriolar tone. *Am J Physiol Heart Circ Physiol* 269:H1590–H1596.